Additional Experimental Results

In the paper, we present quantitative results using mean squared errors between vertex positions or texture values. While these are a natural choice of error metric, in the case of faces there is an attractive alternative. Here we present the same results as in the paper but using angular difference between parameter vectors (in eigenvalue normalised parameter space). This is a model based error which captures differences in the identity component of the face and is invariant to distinctiveness.

3D-3D shape reconstruction

Table 1 shows 3D-3D reconstruction errors (as described in Section 5.1.1) using angular difference as the error measure.

2D-3D Shape reconstruction robustness

In Figure 1 we show reconstruction errors from feature points with different levels of noise. The number of feature points is varied from 10 to 70. The experiment is explained in greater detail in Section 5.1.2 of the main paper.

Face ID	Proposed	RLS	PPCA
001	46.67	52.12	50.24
002	54.64	53.31	64.94
006	49.63	65.70	68.42
014	49.75	57.37	53.41
017	47.77	53.11	46.48
022	57.34	69.37	60.85
052	45.88	53.65	38.86
053	50.22	53.40	50.27
293	39.60	44.36	49.17
323	45.96	48.12	47.75
Mean	48.77	55.09	53.04

TABLE 1: Shape reconstruction errors for 10 out of sample faces. We compare our method to regularised least squares and probabilistic PCA. Errors are angular distance in units of degrees.

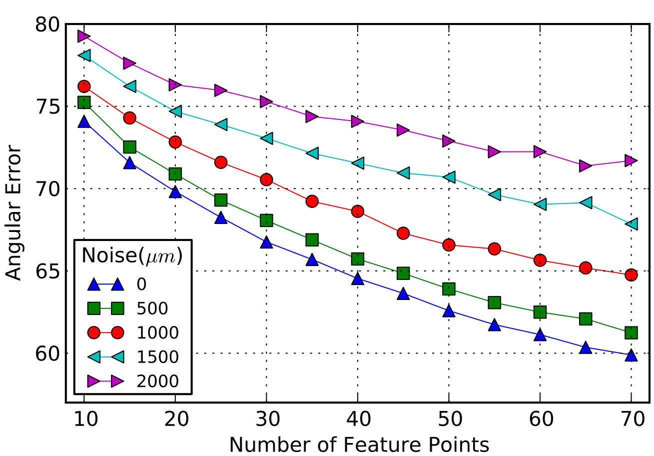

Fig. 1: Shape reconstruction error from 2D feature points, averaged over all subjects. For each number of feature points, the experiment is repeated 20 times with a random subset. The values shown in the figures are mean values.

Pose dependency

To circumvent the effects of perspective distortion in the Basel Face Model renderings, we compare pose accuracy and shape reconstruction for the same set (subjects and pose), rendered with an orthographic projection. Figure 2 shows fitting results for the perspective (left column) and orthographic projections (plots on the right).

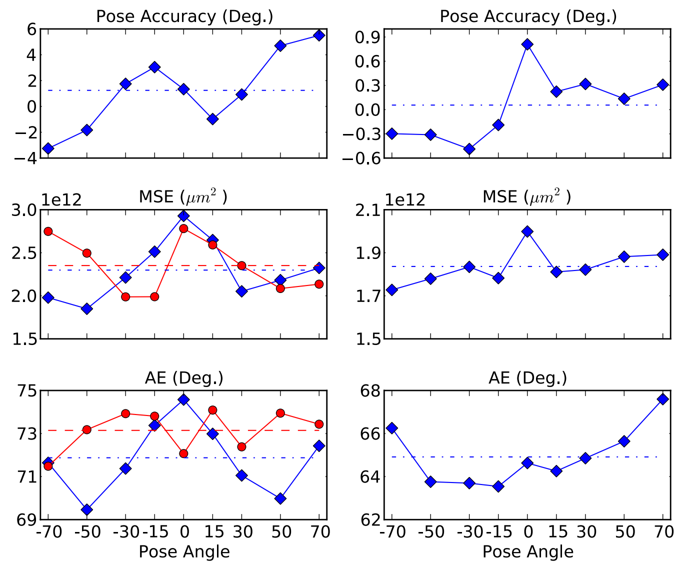

Fig. 2: Left column shows pose and shape accuracy results for perspective renderings. Column on the right shows results for the same setting rendered with an orthographic camera. Results for the proposed method are shown in blue (diamond marker). The red curves (circular marker) show results for [1]. Dashed lines in all plots show mean values.

Rerendering

In Figure 3, we show how the estimated coefficients for shape, pose, texture and illumination are used to rerender the result into the input image. We compare our result with the one obtained by the Multi feature fitting algorithm [1]. For all subjects a novel pose (30 degrees) is shown with the corresponding illumination estimate.

Illumination transfer

To demonstrate the stability of the estimated parameters, we show an example of illumination transfer. We estimate illumination and identity in three images. Illumination is then applied across all subjects. For comparison, we show the ground truth images present in the dataset. The result is shown in Figure 4.

Solution to the Standard Form

In the main paper we express a number of problems in terms of a regularised quadratic form with diagonal distance matrix $\mathbf{\Omega}$ and an optional regularisation term.

Expanding this form gives:

$$
\begin{aligned}
\mathbb{E} &= (\mathbf{Ax}+\mathbf{b})^{\mathrm{T}}\,\boldsymbol{\Omega}\,(\mathbf{Ax}+\mathbf{b}) + \lambda\|\mathbf{x}\| \\
&= \left[(\mathbf{Ax})^{\mathrm{T}}\,\boldsymbol{\Omega} + \mathbf{b}^{\mathrm{T}}\boldsymbol{\Omega}\right](\mathbf{Ax}+\mathbf{b}) + \lambda\|\mathbf{x}\| \\
&= (\mathbf{Ax})^{\mathrm{T}}\,\boldsymbol{\Omega}\mathbf{Ax} + (\mathbf{Ax})^{\mathrm{T}}\,\boldsymbol{\Omega}\mathbf{b} + \mathbf{b}^{\mathrm{T}}\boldsymbol{\Omega}\mathbf{Ax} + \mathbf{b}^{\mathrm{T}}\boldsymbol{\Omega}\mathbf{b} + \lambda\|\mathbf{x}\| \\
&= \mathbf{x}^{\mathrm{T}}\mathbf{A}^{\mathrm{T}}\boldsymbol{\Omega}\mathbf{Ax} + \mathbf{x}^{\mathrm{T}}\mathbf{A}^{\mathrm{T}}\boldsymbol{\Omega}\mathbf{b} + \mathbf{b}^{\mathrm{T}}\boldsymbol{\Omega}\mathbf{Ax} + \mathbf{b}^{\mathrm{T}}\boldsymbol{\Omega}\mathbf{b} + \lambda\|\mathbf{x}\| \\
&= \mathbf{x}^{\mathrm{T}}\mathbf{A}^{\mathrm{T}}\boldsymbol{\Omega}\mathbf{Ax} + \left(\mathbf{A}^{\mathrm{T}}\boldsymbol{\Omega}\mathbf{b}\right)^{\mathrm{T}}\mathbf{x} + \mathbf{b}^{\mathrm{T}}\boldsymbol{\Omega}\mathbf{Ax} + \mathbf{b}^{\mathrm{T}}\boldsymbol{\Omega}\mathbf{b} + \lambda\|\mathbf{x}\|.
\end{aligned}
$$

The solution to the quadratic form with respect to $\mathbf{x}$ is given by:

$$
\begin{aligned}
\frac{\mathrm{d}\,\mathbb{E}}{\mathrm{d}\,\mathbf{x}} &= 2\mathbf{x}^{\mathrm{T}}\mathbf{A}^{\mathrm{T}}\boldsymbol{\Omega}\mathbf{A} + \left(\mathbf{A}^{\mathrm{T}}\boldsymbol{\Omega}\mathbf{b}\right)^{\mathrm{T}} + \mathbf{b}^{\mathrm{T}}\boldsymbol{\Omega}\mathbf{A} + 2\lambda\mathbf{x}^{\mathrm{T}} = 0 \\
&= 2\mathbf{x}^{\mathrm{T}}\mathbf{A}^{\mathrm{T}}\boldsymbol{\Omega}\mathbf{A} + \mathbf{b}^{\mathrm{T}}\left(\mathbf{A}^{\mathrm{T}}\boldsymbol{\Omega}\right)^{\mathrm{T}} + \mathbf{b}^{\mathrm{T}}\boldsymbol{\Omega}\mathbf{A} + 2\lambda\mathbf{x}^{\mathrm{T}} \\
&= 2\mathbf{x}^{\mathrm{T}}\mathbf{A}^{\mathrm{T}}\boldsymbol{\Omega}\mathbf{A} + \mathbf{b}^{\mathrm{T}}\boldsymbol{\Omega}^{\mathrm{T}}\mathbf{A} + \mathbf{b}^{\mathrm{T}}\boldsymbol{\Omega}\mathbf{A} + 2\lambda\mathbf{x}^{\mathrm{T}} \\
&= 2\mathbf{x}^{\mathrm{T}}\mathbf{A}^{\mathrm{T}}\boldsymbol{\Omega}\mathbf{A} + 2\mathbf{b}^{\mathrm{T}}\boldsymbol{\Omega}\mathbf{A} + 2\lambda\mathbf{x}^{\mathrm{T}} \\
&= \mathbf{x}^{\mathrm{T}}\mathbf{A}^{\mathrm{T}}\boldsymbol{\Omega}\mathbf{A} + \lambda\mathbf{x}^{\mathrm{T}} + \mathbf{b}^{\mathrm{T}}\boldsymbol{\Omega}\mathbf{A} \\
&= \left(\mathbf{A}^{\mathrm{T}}\boldsymbol{\Omega}\mathbf{A}\right)^{\mathrm{T}}\mathbf{x} + \lambda\mathbf{x} + \left(\mathbf{b}^{\mathrm{T}}\boldsymbol{\Omega}\mathbf{A}\right)^{\mathrm{T}} \\
&= \mathbf{A}^{\mathrm{T}}\left(\mathbf{A}^{\mathrm{T}}\boldsymbol{\Omega}\right)^{\mathrm{T}}\mathbf{x} + \lambda\mathbf{x} + \mathbf{A}^{\mathrm{T}}\left(\mathbf{b}^{\mathrm{T}}\boldsymbol{\Omega}\right)^{\mathrm{T}} \\
&= \left(\mathbf{A}^{\mathrm{T}}\boldsymbol{\Omega}\mathbf{A} + \lambda\mathbf{I}\right)\mathbf{x} + \mathbf{A}^{\mathrm{T}}\boldsymbol{\Omega}^{\mathrm{T}}\mathbf{b} \\
\mathbf{x} &= -\left(\mathbf{A}^{\mathrm{T}}\boldsymbol{\Omega}\mathbf{A} + \lambda\mathbf{I}\right)^{-1}\left(\mathbf{A}^{\mathrm{T}}\boldsymbol{\Omega}^{\mathrm{T}}\mathbf{b}\right).
\end{aligned}
$$

REFERENCES

[1] S. Romdhani and T. Vetter, "Estimating 3D shape and texture using pixel intensity, edges, specular highlights, texture constraints and a prior," in *Proc. CVPR*, vol. 2, 2005, pp. 986–993.

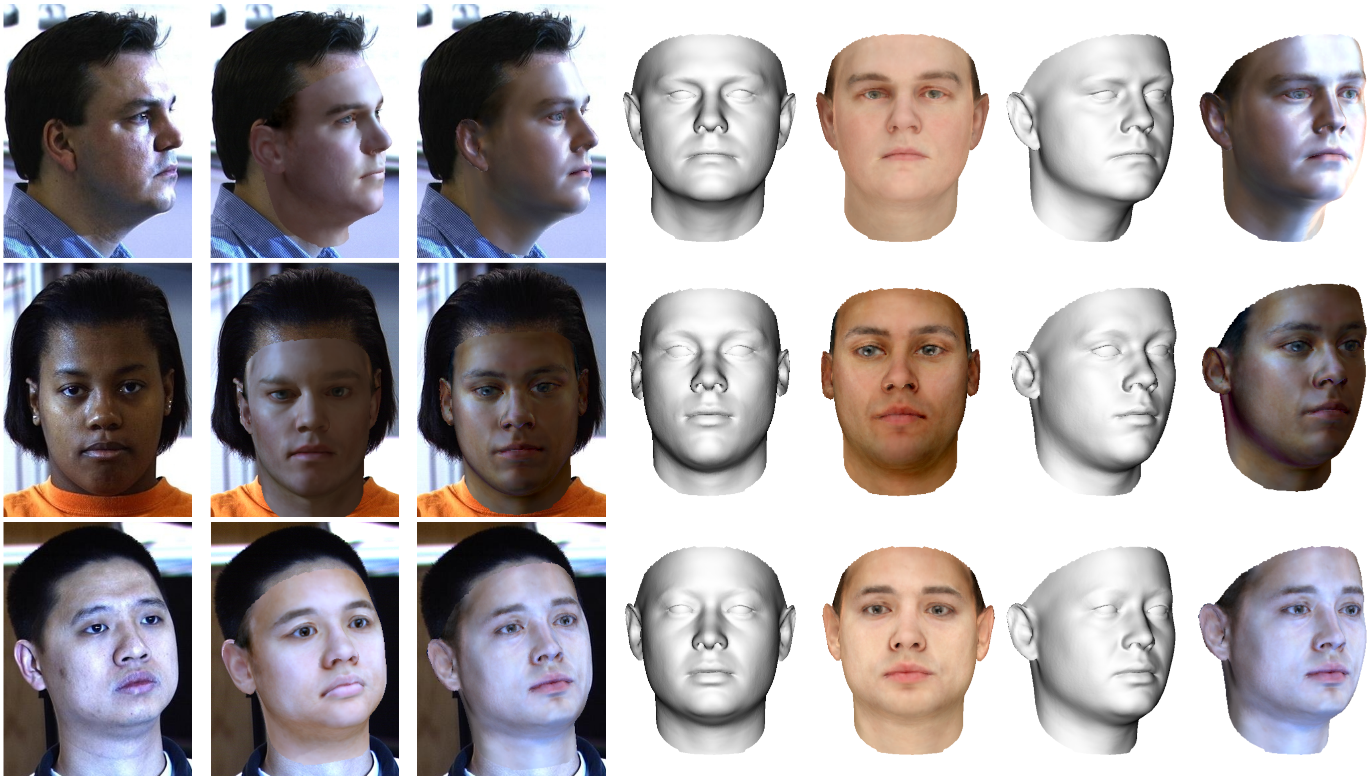

Fig. 3: From left to right: Input Image. Reconstruction rendered into input image [1]. Reconstruction rendered into input image for the proposed method. Shape reconstruction. Shape reconstruction with recovered texture mapped on it. Novel pose (30 deg.). Novel pose with estimated illumination. The second example demonstrates an unavoidable effect when the texture model is put to its limits. In that case, illumination is wrongly estimated in order to reduce overall pixel error.

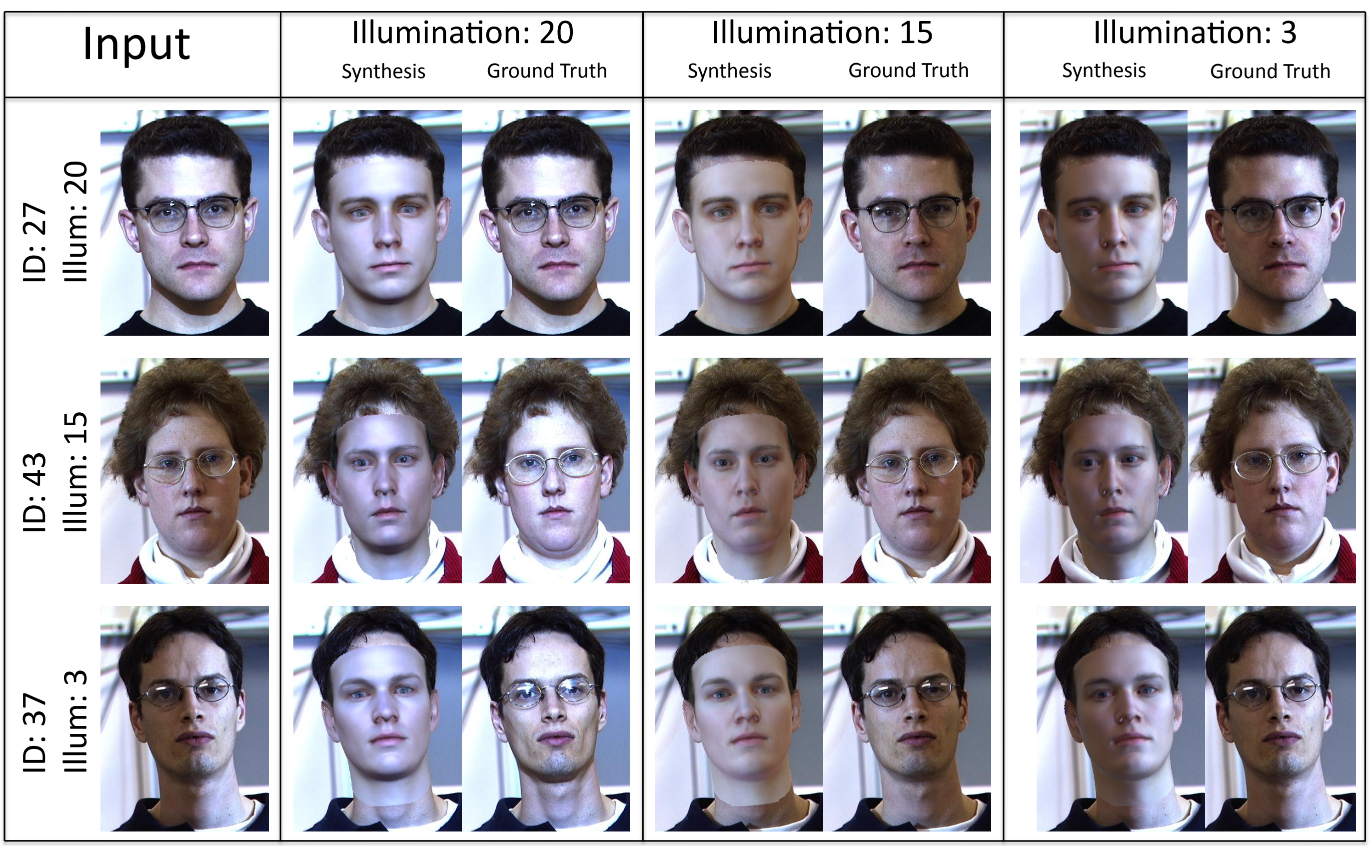

Fig. 4: Illumination transfer example. We estimate identity and illumination in three input images. The illumination is then transferred to all identities and the result rendered into the image. Ground truth is shown for comparison next to the renderings.